A Tactile Element Based on Nonlinear Elasticity to Sense Contact Area

Takayuki Hoshi*, and Hiroyuki Shinoda*

In this paper, we propose a new tactile sensor element to realize robot skins. The sensor element has a large sensing area (several square centimeters) and acquires not only contact force but also contact area. By arraying the sensor elements, we can cover a large area with a small amount of the sensor elements, and collect rich tactile information. The structure of the sensor element is very simple; two layers of isolators (urethane foam) sandwiched by three pieces of stretchable conductive sheets (conductive fabric). The structure enables us to obtain the contact force and the contact area from the capacitances between the conductive pieces. We also propose the method to connect the elements to compose the robot skin including no long wires. CMOS LSI sensor/communication chips are arranged at the boundary of the sensor elements, and the chips measure the capacitances between the conductive layers and send signals through the identical conductive layers.

Keywords : Tactile sensor, Artificial skin, Robot skin, Haptic interface, Contact area, Nonlinear elasticity

1. Introduction

Recently, there is a growing interest in home robots that can care for the aged and young children and that can be alternatives to companion animals. In that situation, robots at home are required to be more cautious about surrounding environments than robots at industrial factories because they interact with humans and there are obstacles and unpredictable events around them. To meet this requisite, robot skins which give tactile sensation to the robots are demanded in robotics [1].

The major requirements for robot skins are following.

- They should cover large areas such as whole surfaces of robots.
- They should sensitively detect rich tactile information related to such as shape, pressure, temperature, and so on.
- They should be soft and stretchable to fit robot surfaces and contact humans safely. Softness is also one of important factors to detect touch feelings.

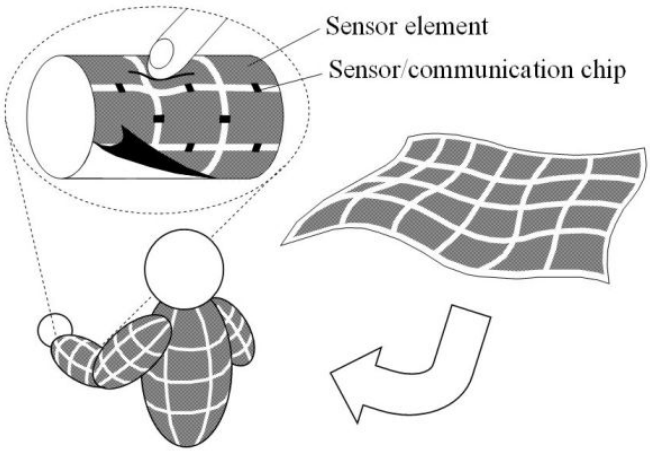

Figure 1. Robot skin composed of proposed sensor elements. It is soft, stretchable, and capable to cover a large area easily.

* Department of Information Physics and Computing, Graduate School of Information Physics and Technology, the University of Tokyo, 7-3-1 Hongo, Bunkyo-ku, Tokyo, Japan 113-8656

In order to realize such a robot skin, various arrays of tactile sensor elements which detect pressure have been tried [2-4]. One approach to enhance the ability of the skin for practical uses is to array the elements in high density. However, we have no practical techniques available now with which we can mount a million of tactile elements with 1 mm spacing in a stretchable sensor skin.

We have proposed a new tactile sensing to solve the problem [5]. In our method, a sensor element has a large sensing area (several square centimeters) and acquires not only contact force but also contact area. Owing to an additional sensing parameter, the contact area, a robot skin which detects minute shape features is easily realized by arraying the elements in low density. In consequence, we can cover whole surfaces of robots with a small amount of the elements (Fig.1). This proposition is based on the characteristics of the human tactile sensation. While Two Point Discrimination Thresholds (TPDT) of humans are several centimeters except on faces and hands, humans can discriminate sharpness of objects sensitively even on such large TPDT parts. From these facts, we suppose that sharpness is one of key components to produce general human tactile sensation [6], and that sensitivity to the sharpness is a high priority for a human-like sensor skin.

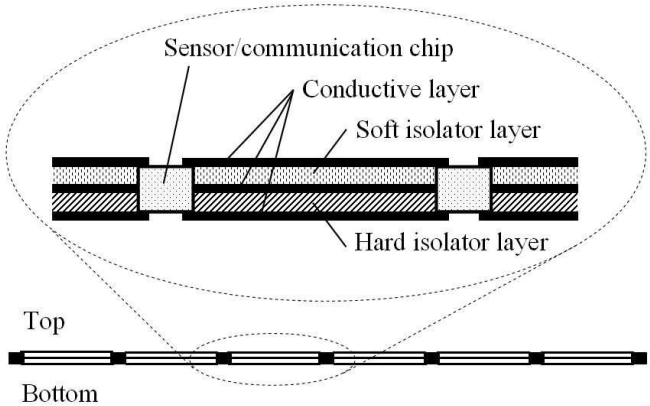

Figure 2. Cross-section of our robot skin. A set of soft and hard layers and three pieces of stretchable conductive sheets form a sensor element.

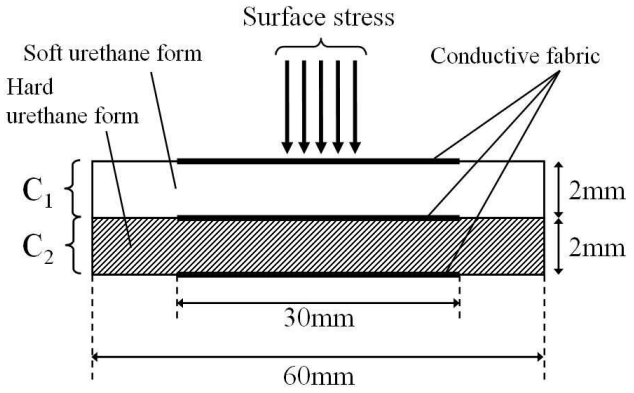

Figure 3. Cross-section of sensor element prototype.

Our sensor element consists of two isolator layers and three pieces of stretchable conductive sheets. In order to acquire the contact force and the contact area, we make use of the nonlinear elasticity of the isolators. The conductive pieces work not only as sensor elements but also as communication paths when CMOS LSI sensor/communication chips are placed at the boundary of the conductive pieces [7], thus wires to sensor elements are no longer needed to realize soft and stretchable skins (Fig.2).

In this paper, we describe the structure and the sensing theory of the sensor element [5]. We show experimental results to examine the feasibility of the method. There are new results that have not been published in [5]. We also explain about the communication method using the CMOS LSI sensor/communication chips to eliminate long wires from the sensor skin.

2. Structure of sensor element

The structure of our sensor element is very simple. In Fig.3, we show schematically the cross-section of the sensor element prototype. The sensor element consists of two isolator layers; the upper layer is made of soft urethane foam (15 kg/m^3) and the lower hard (60 kg/m^3), and each layer is 2 mm in thickness. There are three pieces of stretchable conductive fabric on the soft layer, between the soft and hard, and under the hard, respectively. Each piece has an area of 30×30 mm^2. The side length of the conductive fabric piece is comparable to the TPDT on human forearms. The isolator layers and the conductive pieces are adhered each other by soft double-faced tape. Then two capacitors are formed in the layers. Supposing a surface of a robot body hard, we adhered the bottom of the sensor element prototype to an acrylic base.

3. Sensing theory

We suppose a surface stress as illustrated in Fig.4; a constant surface stress distribution $\sigma(x, y)$ [Pa] is vertically loaded to the surface of the sensor element in a contact field S, that is

$$\sigma(x,y) \equiv \begin{cases} \dfrac{F}{S} & \text{if } (x,y) \in \mathrm{S} \\ 0 & \text{if } (x,y) \notin \mathrm{S} \end{cases} \quad \cdots\cdots (1)$$

where F [N] is the total contact force and S [m^2] is the area of S.

We also assume the following. First, the nonlinear elasticity of the isolator layers is the entropy elasticity [8] expressed as

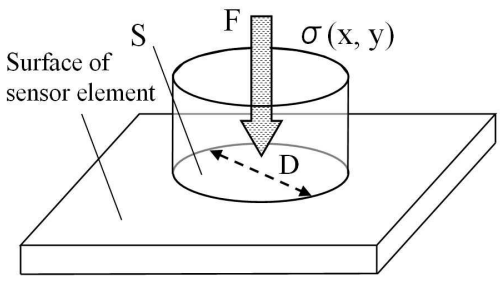

Figure 4. Supposed surface stress distribution $\sigma(x, y)$.

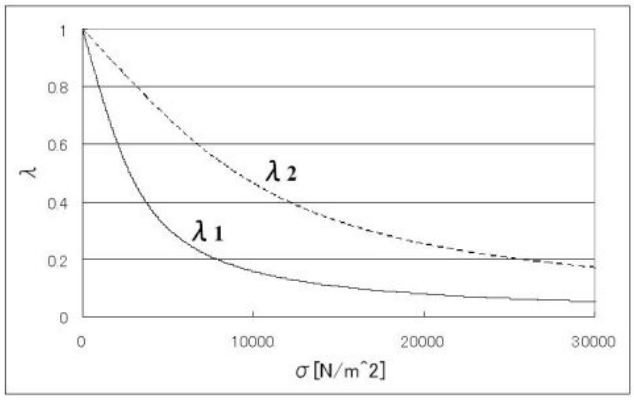

Figure 5. Relationship between surface stress σ and extension ratio λ_n. Soft layer λ_1 is more easily compressed than hard layer λ_2.

$$\sigma = \frac{E_n}{3}\left(\frac{1}{\lambda_n} - \lambda_n^2\right) \quad (n = 1, 2) \quad \cdots\cdots (2)$$

$$\lambda_n \equiv \frac{d_n - \Delta d_n}{d_n} \quad \cdots\cdots (3)$$

where n is the layer identification; n=1 means the upper soft layer and 2 the lower hard layer. E_n [Pa], λ_n and d_n [m] are the elasticity modulus, the extension ratio and the initial thickness of the layer n, respectively. E_1 is about 4,750 Pa and E_2 is 15,400 Pa. The following expression of λ_n (Fig.5) is obtained by solving Eq.(2),

$$\lambda_n = \sqrt[3]{\frac{1}{2} + \sqrt{\frac{1}{4} + \left(\frac{\sigma}{E_n}\right)^3}} + \sqrt[3]{\frac{1}{2} - \sqrt{\frac{1}{4} + \left(\frac{\sigma}{E_n}\right)^3}} \quad \cdots\cdots (4)$$

Second, the conductive pieces have negligible tensions and the Poisson's ratios of the isolator layers are zero, which means that a displacement distribution $\Delta d_n(x, y)$ [m] is determined simply by the local value of $\sigma(x, y)$.

We measure electric capacitances C_n [F] between the conductive pieces to detect $\Delta d_n(x, y)$. Ignoring fringing fields, the capacitances are formulated as

$$C_n = \iint \frac{\varepsilon_n}{d_n - \Delta d_n(x,y)} \mathrm{d}x\mathrm{d}y \quad \cdots\cdots (5)$$

where ε_n is the dielectric constant of the layer n. If we can make the second assumption mentioned above, (C_1, C_2) is uniquely determined by (F, S). Then the key question is whether the inverse

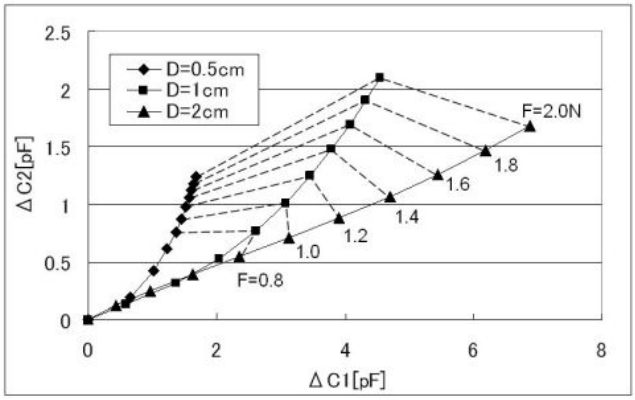

Figure 6. Simulation result. Calculated (ΔC_1, ΔC_2)s for various (F, S)s. D is a parameter defined as $D \equiv 2\sqrt{S/\pi}$ to represent a diameter of S for a circular object.

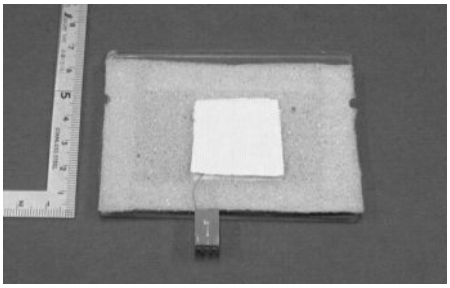

Figure 7. Photograph of sensor element prototype.

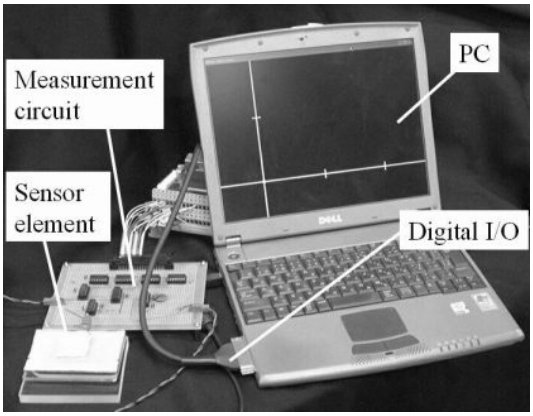

Figure 8. Experimental setup.

mapping from (C_1, C_2) to (F, S) is possible or not for the layers, 1 and 2, having different hardness.

Figure 6 shows the result of a numerical simulation for the elasticity moduli E_1=4,750 Pa and E_2=15,400 Pa. It shows that (ΔC_1, ΔC_2)s for various (F, S)s span a two dimensional space, where (ΔC_1, ΔC_2) are the capacitance differences by the applied force, and D is a parameter defined as

$$D \equiv 2\sqrt{\frac{S}{\pi}} \quad \cdots\cdots (6)$$

to represent the diameter of S for a circular object. It implies that we can determine (F, S) uniquely from (ΔC_1, ΔC_2).

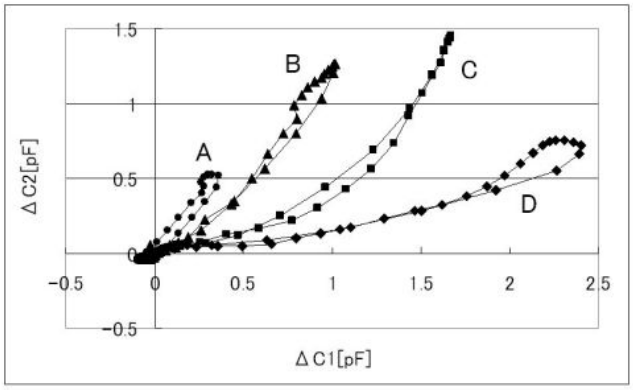

Figure 9. Experimental result for basic performance. Measured trajectories of (ΔC_1, ΔC_2)s for stimulator A: D=0.5 mm, B: D=1 cm, C: D=2 cm, and D: whole area.

4. Experiments and results

We conducted experiments to examine the feasibility of the proposed sensing method. We measured C_n of a sensor element prototype (Fig.7) by a self oscillation method; we generated a RC oscillation including the sensor element as a capacitor, and counted pulses par 2 msec by a 16-bit counter. A PC imported data via a digital I/O, and achieved around 80 Hz effective sampling rate (Fig.8).

4.1 Basic performance This experiment examined whether the sensor element prototype could discriminate four different stimulators; A: D=0.5 mm (as an impulse), B: D=1 cm, C: D=2 cm, and D: whole area. Each stimulator was vertically pressed at the center of the sensor element by hand with force up to around 10 N in 0.5 sec and it was released after that.

In Fig.9, the (ΔC_1, ΔC_2)s during the motion were plotted. It is confirmed possible to discriminate the four stimulators.

4.2 Effect of surface configuration This experiment examined whether the prototype could discriminate the four stimulators A, B, C, and D even when it was placed on the surface of the base with the hemispherical bump shown in Fig.10. As in Section 4.1, each stimulator was vertically pressed at the center of the sensor element by hand with force up to around 10 N in 0.5 sec and it was released after that.

In Fig.11, the (ΔC_1, ΔC_2)s during the motion were plotted. It is also confirmed possible to discriminate the four stimulators when the sensor element is adhered to the curved surface.

4.3 Effect of contact position This experiment examined whether the outputs of the prototype had some relationship with the contact position on the surface of the prototype. We pressed the center and the corners of the sensor element as illustrated in Fig.12 by the stimulator B. We also pressed the center of the sensor element by the stimulators A and C as references. The other conditions were same as the experiment in Section 4.1.

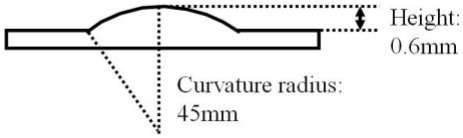

Figure 10. Base with hemispherical bump.

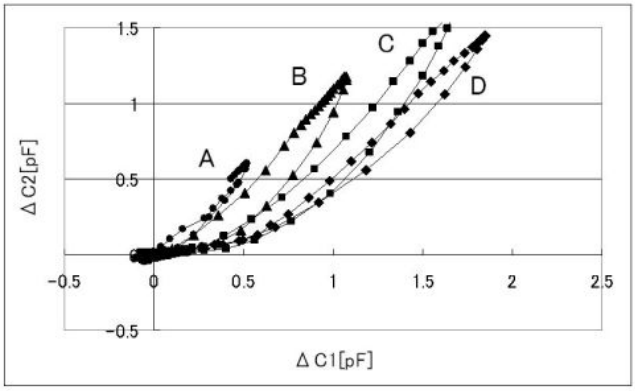

Figure 11. Experimental result for effect of surface configuration. Measured trajectories of (ΔC_1, ΔC_2)s for stimulator A: D=0.5 mm, B: D=1 cm, C: D=2 cm, and D: whole area.

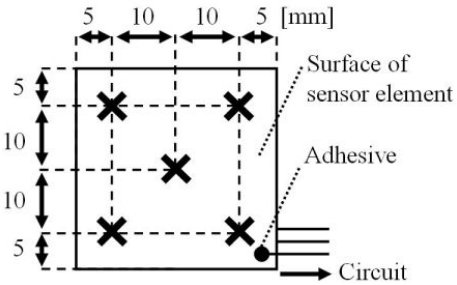

Figure 12. Pressed positions; the center and the four corners.

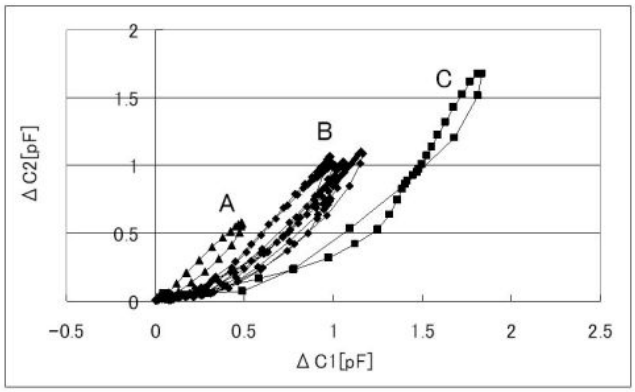

Figure 13. Experimental result for effect of contact position. Measured trajectories of (ΔC_1, ΔC_2)s for stimulator A: D=0.5 mm, B: D=1 cm, and C: D=2 cm.

In Fig.13, the (ΔC_1, ΔC_2)s during the motion were plotted. It is confirmed possible to discriminate the stimulator B from the stimulators A and C regardless of the contact positions.

4.4 Effect of force direction This experiment examined whether the outputs of the prototype had some relationship with the force direction, i.e. the existence of the surface shear stress. We pressed the center of the sensor element by the stimulator A not only vertically but also aslope at an angle of 45 degrees. We also pressed the center by the stimulator B as a reference. The other conditions were same as the experiment in Section 4.1.

In Fig.14, the (ΔC_1, ΔC_2)s during the motion were plotted. It is confirmed possible to discriminate the stimulator A from the stimulator B regardless of the force directions.

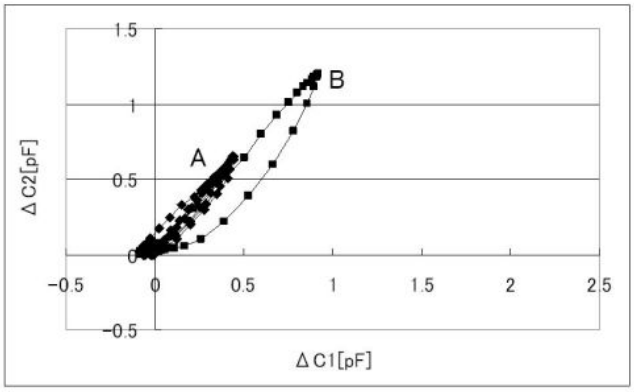

Figure 14. Experimental result for effect of force direction. Measured trajectories of (ΔC_1, ΔC_2)s for stimulator A: D=0.5 mm and B: D=1 cm.

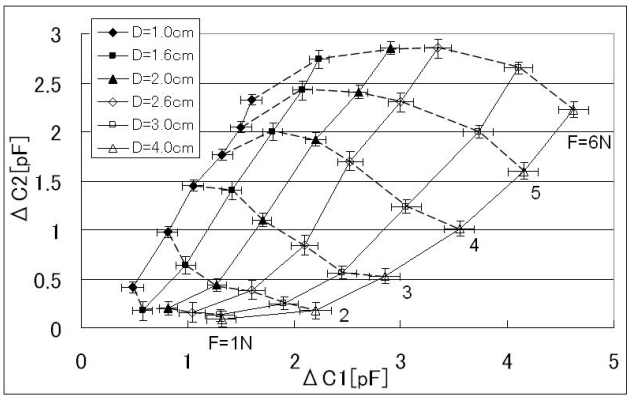

Figure 15. Experimental result for reproducibility. Averaged trajectories of (ΔC_1, ΔC_2)s for various (F, S)s with error bars representing max differences.

4.5 Reproducibility of results This experiment examined whether the outputs of the prototype were reproducible. We used the six stimulators with the diameters D=1.0cm, 1.6cm, 2.0cm, 2.6cm, 3.0cm, 4.0cm, respectively. Each stimulator was vertically pressed at the center of the sensor element by a mechanical setup measuring the pressing force quasi-statically.

In Fig.15, the average (ΔC_1, ΔC_2)s of the 5 trials were plotted with the error bars representing the max differences. It is confirmed that the outputs were almost stable during the 5 trials.

5. Signal transmission

In this research we are developing a sensing chip that senses the capacitance C_n and transmits the signal to the host computer without long wires. Eliminating long wires is crucial to realize a practical elastic sensor skin. In our method, we also use conductive pieces for signal transmission.

At the present stage, we have completed fabrication of the first prototype of CMOS LSI based on 0.35 μm rule for the sensor/communication chip (Fig.16). The total area of the analog-digital mixed circuits is within 1.5 mm^2. The operating frequency of the chip is 50 MHz. Each chip measures C_n with a 8-bit A/D converter and it has a function to transmit the data to the neighboring sensing chip. We have verified the chip can measure the capacitances of one sensor element and transmit data to a PC (Fig.17) successfully. We are in the process of arraying the sensor

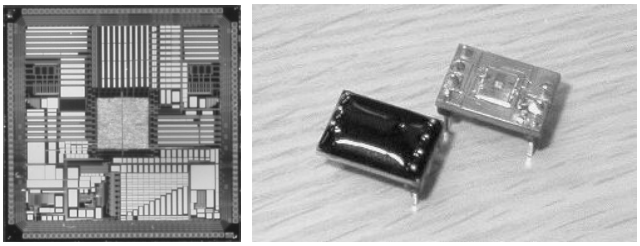

(a) (b)

Figure 16. (a) Close-up top view of current version of CMOS LSI chip. (b) CMOS LSI chip after bonding (right) and molding (left).

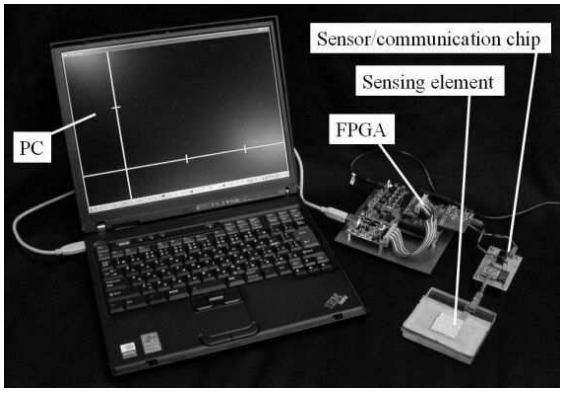

Figure 17. Measurement system using LSI sensor/communication chip.

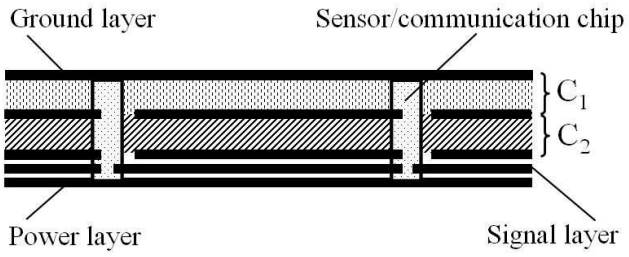

Figure 18. Cross-section of robot skin using current version of LSI chip. The signal layer will be removed in the next version of the prototype.

elements using multiple chips as shown in Fig.18. In the current prototype, five layers of conductive fabric are used. The top conductive layer is used as the ground layer, and bottom two layers are used for the powering and signal layer, under the two layers of sensing pieces. The sensor/communication chips are arranged at the boundary of the sensor elements. The data packets are multi-hopped through the signal layer. The signal layer will be removed in the next version of the prototype in which the chips also transmit signals through the sensing pieces.

6. Conclusion

In this paper, we proposed a new tactile sensor element using the nonlinear elasticity to acquire not only contact force but also contact area. This sensing method is based on the characteristics of the human tactile sensation. We also introduced a communication method in which the conductive pieces of the sensor elements are also used as the signal transmission layers. By combining these two technologies, we can achieve soft and stretchable robot skins which detect minute shape features of contact objects, and cover whole surfaces of robots.

Acknowledgement

We thank Naoya Asamura, Tachio Yuasa, Mitsuhiro Hakozaki, Xinyu Wang, and Hiroto Itai, Cellcross Co., Ltd. for their cooperation on fabricating and evaluating the prototype of the CMOS LSI chip, and providing ideas on device structures and their applications.

References

(1) M. H. Lee, and H. R. Nicholls : “Tactile sensing for mechatronics - a state of the art survey”, Mechatronics, Vol. 9, pp. 1-31 (1999)

(2) Y. Hoshino, M. Inaba, and H. Inoue : “Model and Processing of Whole-body Tactile Sensor Suit for Human-Robot Contact Interaction”, Proc. of the 1998 IEEE International Conference on Robotics & Automation (ICRA '98), pp. 2281-2286 (1998)

(3) R. Kageyama, S. Kagami, M. Inaba, and H. Inoue : “Development of Soft and Distributed Tactile Sensors and the Application to a Humanoid Robot”, Proc. of the IEEE International Conference on Systems, Man, and Cybernetics, Vol. 2, pp. 981-986 (1999)

(4) O. Kerpa, K. Weiss, and H. Worn, “Development of a Flexible Tactile Sensor System for a Humanoid Robot”, Proc. of the 2003 IEEE/RSJ International Conference on Intelligent Robots and Systems (IROS 2003), Vol. 1, pp. 1-6 (2003)

(5) T. Hoshi, and H. Shinoda, “Tactile Sensing Using Nonlinear Elasticity”, Proc. SICE Annual Conference 2005, pp. 2978-2981 (2005)

(6) Y. Makino, N. Asamura, and H. Shinoda, “Multi Primitive Tactile Display Based on Suction Pressure Control”, Proc. IEEE 12th Symposium on Haptic Interfaces for Virtual Environment and Teleoperator Systems (Haptic Symposium 2004), pp. 90-96 (2004)

(7) A. Okada, Y. Makino, and H. Shinoda, “Cell Bridge: A Signal Transmission Element for Networked Sensing”, Proc. SICE Annual Conference 2005, pp. 3826-3831 (2005)

(8) G. R. Strobl, “The Physics of Polymers: Concepts for Understanding Their Structures and Behavior”, Springer (1997)